RSC Advances

PAPER

View Article Online
View Journal | View Issue

Cite this: *RSC Adv.*, 2025, **15**, 4915

ZIP-8/Ag-based size-selective SERS nanoplatform for ultrasensitive urea detection in milk samples: effects of analyte molecular dimensions on adsorption capacity and sensing performance†

Dao Thi Nguyet Nga,‡[a] Quan Doan Mai,[a] Linh Ho Thuy Nguyen,[bc] Tan Le Hoang Doan,[bc] Vu Thi Kim Oanh,[d] Ta Ngoc Bach,[d] Vu Dinh Lam,[d] Ha Anh Nguyen ‡*[a] and Anh-Tuan Le *[a]

Being well-known as an excellent sorbent, metal–organic frameworks (MOFs) have been employed to intergrate with noble metal nanoparticles to fabricate active substrates for surface-enhance Raman spectroscopy (SERS) sensing applications. In this work, we employed three organic molecules with different molecular dimensions, including urea, methylene blue (MB) and Congo red (CR) for investigating SERS performance of a ZIP-8/Ag heterostructure. While every dimension of urea is smaller than the pore size of ZIP-8, MB and CR has one dimension larger than that of the pore size. The results show that only urea experienced large SERS enhancements on ZIP-8/Ag sensing platform. In contrast, MB and CR exhibited lower SERS intensity on ZIP-8/Ag than on pure Ag nanoparticle substrates. Adsorption capacities of those analyte were then calculated to confirm that urea could be adsorbed into ZIP-8/Ag at the best rate. The size-dependent mechanism of analyte adsorption and improving SERS signal was then confirmed using two other organic compounds: 4-nitrophenol (4-NP) and chloramphenicol (CAP). Thanks to the size-selective adsorption, small molecules such as urea and 4-NP can be effectively detected in the presence of large interfering molecules, which is useful for developing advanced SERS applications. The ZIP-8/Ag-based SERS sensor could detect urea at impressive concentrations as low as 1.48×10^{-10} M in standard solutions and 10^{-8} M in milk.

Received 28th October 2024
Accepted 6th February 2025

DOI: 10.1039/d4ra07695h

rsc.li/rsc-advances

1. Introduction

Surface-enhanced Raman spectroscopy (SERS) has been regarded as a powerful molecular analytical tool that allows rapid and highly sensitive detection of chemical and biological compounds based on the characteristic vibration of their bonds.[1,2] Noble metal nanoparticles (NPs), such as Au, Ag, Cu, *etc.*, are usually employed as SERS active substrates, thanks to localized surface plasmon resonance (LSPR) on their surface.[3,4] To be detailed, the resonance coupling between the incident laser at certain wavelengths and the metal substrate occurs and forms a strong electromagnetic field, leading to enormous enhancement of Raman signal of the analytes absorbed on the surface of the substrate.[2,5] As a result, the SERS signal can be collected, reflecting its presence in the analytical samples. On one hand, the close distance between the analyte and the metal surface allows it to experience the strong electromagnetic field to promote SERS enhancement in electromagnetic mechanism.[2,5] On the other hand, the close distance is convenient for charge transfer, which is the main principle of chemical SERS enhancement.[2,6] Therefore, in the effort of improving SERS sensing systems, researchers have designed and developed different SERS substrates for better adsorption of analytes. In addition to the key materials of noble metal NPs, the incorporation of sorbent components such as graphene oxide[7,8] and different semiconductors including MnO_2,[9,10] ZnO,[11] TiO_2,[12] *etc.*, leading to detection of various organic compounds at impressive detection limit. More recently, intergrating noble metal NPs with porous structures to create hybrid materials has been a promising approach to develop effective SERS active substrates.

Metal–organic frameworks (MOFs) are is a kind of porous crystalline material created by the self-assembly of metal ions or

[a]*Phenikaa University Nano Institute (PHENA), Phenikaa University, Hanoi 12116, Vietnam. E-mail: anh.nguyenha@phenikaa-uni.edu.vn; tuan.leanh@phenikaa-uni.edu.vn*

[b]*Center for Innovative Material and Architectures, Ho Chi Minh City, Vietnam*

[c]*Vietnam National University-Ho Chi Minh City, Ho Chi Minh City, Vietnam*

[d]*Institute of Materials Science (IMS), Graduate University of Science and Technology (GUST), Vietnam Academy of Science and Technology, 18 Hoang Quoc Viet, Hanoi 10000, Vietnam*

† Electronic supplementary information (ESI) available. See DOI: https://doi.org/10.1039/d4ra07695h

‡ D. T. N. Nga and H. A. Nguyen contributed equally to this work.

clusters and organic molecules as nodes and ligands, respectively.[13,14] Thanks to its superior porosity, great chemical stability, large specific surface area and good tunability, MOFs shows a wide range of applications including molecular adsorption,[15,16] separation,[17,18] and storage.[15,17] Therefore, MOFs are promising sorbent materials to combine with noble metal NPs to generate hybrid SERS substrates, in which analytes can be adsorbed into the porous structure of MOF, leading to the increase of local concentration of the analyte around the noble metal NPs. Consequently, more molecules can experience SERS effect generated around the NPs in the excitation of the laser, resulting in the improvement of SERS signal of the targeting molecules. Hence, MOFs – noble metal SERS platforms have been employed to develop sensing systems for various analytes, using different types of MOFs. For example, Cai *et al.* fabricated a core–shell SERS platform with AuNPs as the core and MIL-101 as the shell. This structure allowed methenamine to be adsorbed onto the substrate, resulting in a detection limit (LOD) of 5.0×10^{-10} M.[19] A similar strategy have been applied to prepare another Au@ZIF-8 core–shell NPs in a study of Li's group to sense 3 different VOCs, including toluene, chlorobenzene and ethylbenzene.[20] However, in a 2022 study, Yang *et al.* claimed that the full encapsulation of MOF layer around noble metal NP in those structures is inconducive to energy collecting and exchanging, therefore, they developed an un-fully encapsulated core–shell structure with Ag nanowires and ZIP-8, leaing to detection of two water-insoluble pesticides methylparathion and carbaryl with LODs as low as 7.6×10^{-9} M and 5.7×10^{-9} M, respectively.[21] Similar heterostructures with the cores of nanowires were established to generate SERS sensors for CO_2 (ref. 22) as well as thiram and melamine.[23] In another strategy, MOFs have also become a platform for NPs decoration. Zhang *et al.* introduced a corn-like Ag@carbon structure consisting of AgNPs decorated on a carbonated MOF platform, resulting in the formation of fixed spacing distance of AgNPs of 7 nm to generate SERS hot spot to enhance Raman intensity of three organic dyes (*i.e.*, methylene blue (MB), malachite green and crystal violet).[24] Although there have been various combinations of metal NPs and MOFs fabricated using different strategies, targeting analytes of distinct natures, each study often focused on one type of analytes such as VOCs, gases, organic dyes, pesticides, *etc.* Meanwhiles, the efficiency of MOF as a sorbent platform may vary with different analytes. Unfortunately, there was few discussion on the differences in SERS enhancement of different analytes on one certain metal-MOF heterostructure to clarify the effect of different analytes on SERS performance of a metal-MOF sensing platform.

Inspired by the aforementioned ideas, in this study, we prepared SERS active substrates based on ZIP-8/Ag for the detection of several organic analytes with different molecular dimensions, including urea ($3.0 \times 4.97 \times 5.34$ Å),[25] MB ($17.0 \times 7.6 \times 3.3$ Å)[26] and Congo red (CR) ($1.4 \times 9.3 \times 21.0$ Å).[27] Among those, urea has been illegally added into dairy products to inflate their protein contents, which may cause kidney diseases in human. MB and CR are widely used dyes, which are carcinogenic and non-biodegradable. Therefore, they have been targets for SERS detections. On the other hand, ZIP-8 framework exhibited the pore size of 11.6 Å as reported in previous studies.[28–30] SERS measurements of those analyte showed differences in SERS enhancements of distinct analytes. While SERS signals of urea at different concentrations on ZIP-8/Ag were significantly improved in comparison to those on pure AgNPs, SERS signals of larger molecules at different concentrations on ZIP-8/Ag were even lower than those on pure AgNPs. It suggested that to be effectively adsorbed onto the Ag/ZIP-8 substrate, the analyte should be smaller that the ZIP-8 pore size at every dimension. The adsorption rates of the analytes onto Ag/ZIP-8 was confirmed by absorption spectra. Thanks to the differences in SERS enhancement in the presence of ZIP-8, the heterostructure was a size-selective SERS substrate for detection of organic compounds and ZIP-8 worked as a size-filter for the adsorption of analytes. It was convenient to develop SERS sensors for real samples, which contained large organic molecules. On ZIP-8/Ag heterostructure, urea was detected at concentrations as low as 1.48×10^{-10} M in standard solutions and 10^{-8} M in milk samples. The study proposed a size-selective mechanism for Ag/ZIP-8 SERS substrate and suggested a quick step to determine if the targeting analyte was suitable for the SERS sensing system. This time-saving strategy could be convenient for researchers who would like to develop metal-MOF SERS substrates, which requires effective adsorption of analytes into the MOF matrix.

2. Materials and methods

2.1. Materials and SERS substrates

2-Methylimidazole, zinc nitrate hexahydrate ($Zn(NO_3)_2 \cdot 6H_2O$, >98%), polyvinylpyrrolidone (PVP), sodium citrate ($Na_3C_6H_5O_7$, 99.9%), urea, methylene blue, Congo red, 4-nitro phenol and chloramphenicol, purity >98%, were purchased from Sigma-Aldrich Chemical Company (USA). Two silver plates (purity 99.99%) were prepared with dimensions of 100 mm × 5 mm × 0.5 mm. All chemicals were at analytical reagent grade and were used without further purification. In addition, double-distilled water was used in all experiments.

Aluminum (Al) substrates were fabricated as described in our previous study with dimensions of 1 cm × 1 cm × 0.2 cm with a surface-active area with a diameter of 0.2 cm.[31] The substrates were immersed in a diluted hydrochloric acid solution to remove the oxides/hydroxides on the surface, washed with ethanol and double distilled water in an ultrasonication bath for 15 min, then dried naturally at room temperature.

2.2. Synthesis of ZIF-8 and AgNPs

ZIF-8 was prepared using the solvothermal method with polyvinylpyrrolidone (PVP) as a modulator. In a typical procedure, 892 mg of $Zn(NO_3)_2 \cdot 6H_2O$ (4.37 mmol) and 493 mg of 2-methylimidazole (6.00 mmol) were dissolved in 100 mL of ethanol, followed by constant stirring at room temperature. After 20 min of stirring, 687.5 mg of PVP was added into the solution, followed by 6 h of continuous stirring. The product (ZIP-8) was collected by centrifugation at 16 000 rpm for 15 min, washed

with ethanol, and then subjected to evacuation at 80 °C for 24 h under vacuum.

AgNPs were prepared *via* a facile electrochemical method in 0.1% sodium citrate as described in our previous study.[32,33] Two clean silver plates were placed vertically face to face as two electrodes. Electrolysis was undertaken at room temperature under uniform magnetic stirring at 200 rpm for 2 h.

2.3. Preparation of ZIF-8/Ag

ZIF-8/Ag nanocomposites were synthesized using a simple physical mixing method. 15 mg of ZIF-8 powder was distributed in 15 mL of double-distilled water under uniform stirring for 30 min and mixed with 15 mL of AgNP solution. Subsequently, magnetic stirring at high rate for 30 min was required to ensure a homogeneous distribution of the components (500 ppm).

2.4. Characterizations and measurements

The microscopic morphology and structure were analyzed by scanning electron microscopy (SEM, Hitachi S-4800) operated at an acceleration voltage of 5 kV. Ultraviolet-visible (UV-vis) absorption spectra of obtained materials were recorded using a JENWAY 6850 double-beam spectrophotometer with 10 mm-path length quartz cuvettes. Power X-ray diffraction (XRD, BrukerD5005 X-ray diffractometer) with strictly monochromatized Cu Kα ($\lambda = 1:5406$ Å) under a voltage of 40 kV and a current of 30 mA was utilized to identify the phase and chemical composition of the samples. The composition and chemical properties were monitored by Raman spectroscopy (Horiba Macro-RAM™) with 785 nm laser excitation.

Urea, MB, CR, 4-NP and CAP solutions (5 μL) with various concentrations were directly drop-casted onto the prepared substrates and dried naturally at the temperature room before the SERS measurement. The SERS spectra were collected using with a MacroRaman™ Raman spectrometer (Horiba) equipped with a 100× objective with a numerical aperture of 0.90, at a focal length of 115 nm, using the laser power 45 mW at a 45° contact angle. An exposure time of 10 s was used with three accumulations.

Milk was purchased from a local supermarket in Hanoi (Vietnam). Urea-spiked milk was prepared by adding an appropriate volume of urea standard solution into the milk. Subsequently, the spiked milk was drop-casted directly on the prepared substrates for SERS measurements.

2.5. Adsorption of urea, MB and CV into/onto ZIP-8/Ag matrix

The adsorption level of urea, MB and CV into ZIP-8/Ag matrix was evaluated using UV-vis spectroscopy. 10 μL of analyte solution (5 mM) added into 2.0 mL of ZIP-8/Ag solution (50 ppm). Adsorption spectra of the samples were recorded right after the addition and after 5 min, 10 min, 20 min, 30 min and so on, until the intensity of the absorption band each compound achieved a steady state.

3. Results and discussion

3.1. Characteristics of ZIP-8/Ag

Fig. 1a shows SEM images of ZIF-8 in a uniform crystal morphology with good size distribution with the mean diameter of about 100 nm without any obvious aggregation. Besides, the ZIP-8 particles exhibit a relatively smooth surface. Full characterization of ZIP-8, including X-ray diffraction (XRD), Fourier-transform infrared (FT-IR), thermal gravimetric analyses (TGA) and pore size calculation of around 11 Å were established in our previous report.[28] Even in the addition of AgNPs, the ZIF-8 structure remained intact (Fig. 1b). AgNPs with the size of approximately 20 nm have been attached on the ZIP-8 nanostructure, forming a rougher surface, which is promising to generate promising SERS effect. The size of AgNPs is in good agreement with our previous study.[31] The size of AgNPs is also so large that they cannot be loaded into the MOF structures. As the composite was prepared *via* physical mixing method, AgNPs could only attach onto the surface of ZIP-8 frames.

Fig. 1c shows Raman spectrum of ZIP-8/Ag in comparison with that of ZIP-8. The Raman spectrum of ZIP-8 exhibit various peaks at 685 cm^{-1}, 836 cm^{-1}, 953 cm^{-1}, 1022 cm^{-1}, 1146 cm^{-1}, 1180 cm^{-1}, 1348 cm^{-1}, 1460 cm^{-1}, 1500 cm^{-1}, 1510 cm^{-1} and 2924 cm^{-1}. Most of those bands, including 836 cm^{-1}, 953 cm^{-1}, 1022 cm^{-1}, 1180 cm^{-1}, 1384 cm^{-1}, 1500 cm^{-1}, 1510 cm^{-1} and 2924 cm^{-1}, was assigned to methyl group and imidazole ring vibrations (Table S1†). The bands at 685 cm^{-1}, 1146 cm^{-1} and 1460 cm^{-1} was associated with imidazolium ring puckering, C–N and methyl bending, respectively.[34] In the presence of Ag, the Raman spectrum show an intense sharp band at around 300 cm^{-1}, corresponding to Ag–O stretching, representing the presence of AgNPs in the matrix. As the ZIP-8 structure stayed intact in the addition of AgNPs, the characteristic bands of ZIP-8 still remains. However, due to the high intensity of the band at 300 cm^{-1}, those bands look less intense. However, the bands at 685 cm^{-1}, 953 cm^{-1}, 1022 cm^{-1}, 1384 cm^{-1}, 1500 cm^{-1} and 2924 cm^{-1} could still be observed in this spectrum.

3.2. Effects of molecular dimensions of analytes on SERS performance of ZIP-8/Ag: an explanation based on adsorption capacity

To investigate the effect of molecular dimensions of analytes on SERS efficiency of ZIP-8/Ag, three organic compounds with different properties have been selected, including urea, MB and CR. First, urea is a small molecule with dimensions of 3.0 × 4.97 × 5.34 Å,[25] in which every dimension is smaller than the pore size of ZIP-8 of 11.6 Å.[28–30] Urea is not charged, but it is highly polar. The other compounds were MB with the dimensions of 17.0 × 7.6 × 3.3 Å,[26] and CR with the dimensions 1.4 × 9.3 × 21.0 Å.[27] Each compound has one dimension larger than the pore size of ZIP-8. Besides, while MB is negatively charged in solution, CR is positively charged. SERS signals of urea, MB and CR at different concentrations was recorded on two SERS substrates: pure AgNPs and ZIP-8/Ag for comparison purpose.

Fig. 2a–c display SERS spectra of urea on ZIP-8/Ag in comparison with those on pure AgNPs. Urea has been reported

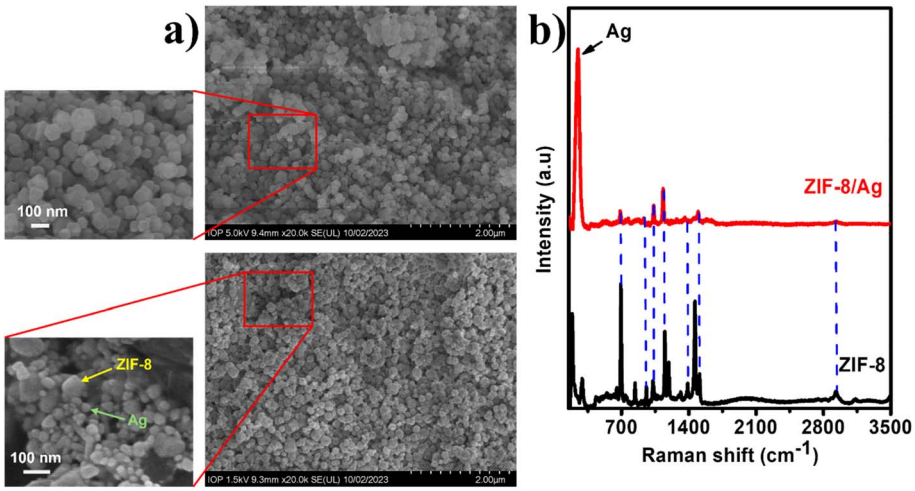

Fig. 1 (a) and (b) SEM images of ZIF and ZIF/Ag, respectively; (b) Raman spectra of ZIF-8 and ZIF-8/Ag.

to be a low Raman cross-section molecules, resulting in its low SERS signal on many substrates.[35,36] Urea molecule contains only one carbonyl group (>C=O) and two amino groups ($-NH_2$). As a result, at the concentration of 10^{-3} M, the presence of urea absorbed on AgNPs is reflected in the SERS spectrum with only one characteristic band at 1010 cm^{-1}, representing C–N stretching mode (Fig. 2a). However, the SERS intensity at this band is relatively low of about 500 a.u. In the incorporation of ZIP-8 into the SERS substrate to create ZIP-8/Ag, the SERS intensity is significantly improved. The SERS intensity of urea (10^{-3} M) on ZIP-8/Ag at the band of 1010 cm^{-1} is approximately 9 times higher than that on pure AgNPs. Similarly, at the concentration of 10^{-4} M, while the SERS intensity of urea on AgNPs is even lower, the SERS spectrum of this analyte on ZIP-8/Ag still exhibits a characteristic band. Furthermore, at concentration as low as 10^{-5} M, there is no band detected in the SERS spectrum of urea on AgNPs. However, the SERS spectrum of urea on ZIP-8/Ag still reflects the presence of urea in the sample with a clear peak at 1010 cm^{-1}. Hence, using ZIP-8/Ag as the substrate, the SERS signal of urea have been enhanced obviously, compared to the use of pure AgNPs.

Similarly, SERS spectra of MB at different concentrations (10^{-5} to 10^{-7} M) were also recorded on AgNPs and ZIP-8/Ag substrates. On AgNPs, SERS spectrum of MB (10^{-5} M) shows sharp and intense peaks at 450 cm^{-1}, 1315 cm^{-1}, 1420 cm^{-1} and 1613 cm^{-1}. The peak at 450 cm^{-1} was assigned for skeletal deformation vibration of C–N–C, respectively. The band at 1315 cm^{-1} was associated with the $N–O_2$ symmetric stretching vibration. The bands at 1420 cm^{-1} and 1620 cm^{-1} were corresponding to stretching modes of C–N and C–C ring, respectively.[37–39] In the presence of ZIP-8 in the SERS substrate, we observed a significant decrease in SERS intensity at every characteristic band as shown in Fig. 3a. At the band of 450 cm^{-1}, at which the SERS intensity of MB is usually employed to calculate its concentration in several previous studies, the SERS intensity of MB on AgNPs is nearly 3.5 times higher than that on ZIP-8/Ag. A similar trend was also observed at the two other concentrations of MB, including 10^{-6} M (Fig. 3b) and 10^{-7} M (Fig. 3c). At the lowest concentration of 10^{-7} M, on ZIP-8/Ag, the characteristic band could be rarely detected on the SERS spectrum while still being obvious in the SERS spectrum of the analyte on AgNPs. Hence, the modification in material did not lead to any improvement in SERS performance of the substrate. In contrast, it reduced the SERS intensity of MB, and therefore, lowered the detection ability of the sensing platform.

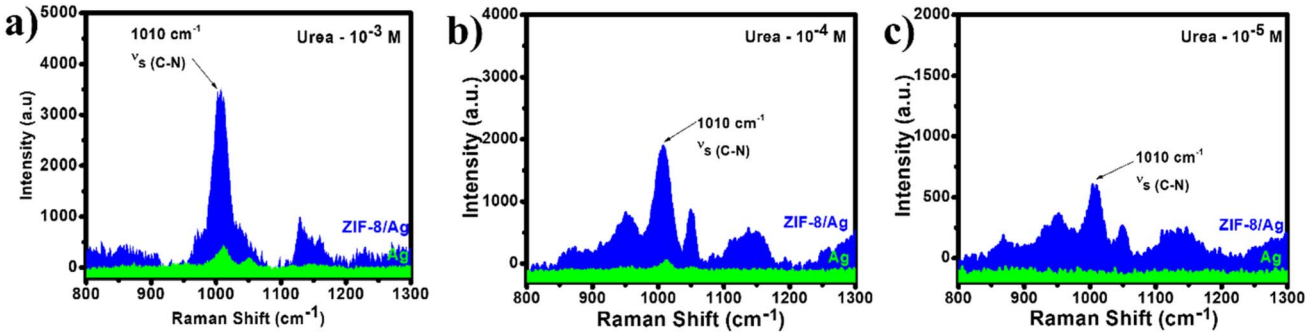

Fig. 2 SERS spectra of urea at 10^{-3} M (a), 10^{-4} M (b) and 10^{-5} M (c) on AgNPs and ZIP-8/Ag substrates.

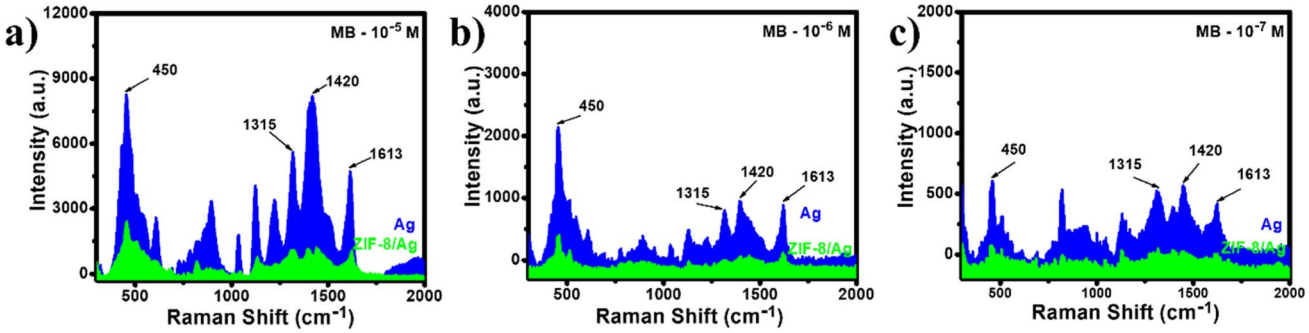

Fig. 3 SERS spectra of MB at 10^{-5} M (a), 10^{-6} M (b) and 10^{-7} M (c) on AgNPs and ZIP-8/Ag substrates.

Concerning another organic dye, CR, Fig. 4a shows the SERS spectrum of CR (10^{-4} M) on ZIP-8/Ag in comparison to that on AgNPs. Similar to the case of MB, SERS spectrum of CR on AuNPs exhibits sharp peaks at 1150 cm^{-1}, 1270 cm^{-1}, 1450 cm^{-1} and 1600 cm^{-1}. The band at 1150 cm-1 was assigned to asymmetric stretching of N–N groups. The band at 1270 cm^{-1} was associated with hydrazone C–N– stretching vibrations. The bands at 1450 cm^{-1} and 1600 cm^{-1} were related to C=C and C–C stretching of the aromatic ring, respectively.[40] On ZIP-8/Ag, the peaks are relatively indistinct, and the peak at 1450 cm^{-1} is nearly undetectable. Moreover, the SERS intensity of CR on ZIP-8/Ag is also lower than that on AgNPs. For example, at the peak of 1270 cm^{-1}, the SERS intensity of CR on AgNPs is around 1.7 times higher than that on ZIP-8/Ag. At the lower concentration of 10^{-5} M, on AgNPs, several peaks of CR can be detected at low intensity in the SERS spectrum while the presence of CR can not be confirmed through its SERS spectra on ZIP-8/Ag (Fig. 4b). At the lowest concentration of 10^{-6} M, no characteristic peak is detectable in both spectra (Fig. 4c). Once again, the incorporation of ZIP-8 in the Ag-based SERS substrate did not improve its SERS sensing performance.

Our previous studies claimed when coated on Al substrates, AgNPs that were synthesized using electrochemical methods could self-assemble to form close interparticle distance of 3–5 nm.[31,41] This distance generates large enhancements in SERS signal of the analytes, leading to the appearance of the sharp peaks in the SERS spectra of MB (10^{-5} M) and CR (10^{-4} M) on AgNPs. Moreover, even a low Raman cross-section as urea could exhibit its characteristic band clearly on this substrate. By intergrating with ZIP-8 in the nanocomposite material, we sacrificed this self-assembly as AgNPs could not distribute as uniformly and create such interparticle distance on the surface of ZIP-8. It could be the reason for its poor SERS performance while sensing MB and CR. However, the presence of ZIP-8 in the SERS substrate did not always reduce the SERS performance of the sensing platform. In fact, SERS signal of urea on ZIP-8/Ag has been significantly improved, compared to the use of pure AgNPs. It could allow urea to be detected at a low LOD, which will be calculated in the following section. ZIP-8 and other MOF structures are well-known sorbent materials which can adsorb analytes into its matrix as a step of preconcentrating before SERS measurement, leading to enhancement of SERS signal. Thus, the adsorption could have been the key for the improvement in urea sensing performance of ZIP-8/Ag, in comparison to the other analytes. The adsorption of urea, MB and CR into ZIP-8/Ag was investigated *via* an absorption model in Section 2.5. The changes over time in the absorption intensity of urea solution in the presence of ZIP-8/Ag were displayed in Fig. S1† (right). With the increase of incubation time, the characteristic absorption band of urea at 200 nm decreases, representing the adsorption of urea into the ZIP-8/Ag matrix. Similarly, the changes over time in the absorption intensity of MB and CR solutions in the presence of ZIP-8/Ag were shown in Fig. S2b and S3b,† respectively. However, absorption spectra of MB and CR does not change significantly during incubation time. Using the absorption intensity obtained at 200 nm for urea, 663 nm for

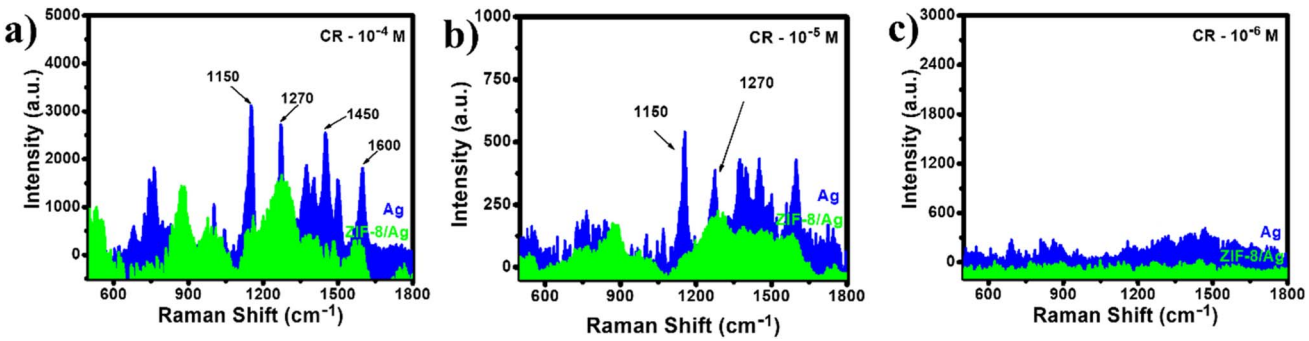

Fig. 4 SERS spectra of CR at 10^{-4} M (a), 10^{-5} M (b) and 10^{-6} M (c) on AgNPs and ZIP-8/Ag substrates.

MB and 498 nm for CR, the concentration of each compound was calculated using the Beer–Lambert law:

$$A = \varepsilon lc \quad (1)$$

in which A is the absorption intensity, ε is the molar absorption coefficient (L mol^{-1} cm^{-1}); l is the optical path length (cm); and c is concentration of the solution (mol L^{-1}). The molar absorption coefficients for urea, MB and CR are the slope of the plot in Fig. S1a, S2a and S3a,† respectively.

Fig. 5 shows the changes in concentration of urea, MB and CR in the solution over incubation time. Concerning urea, over the 90 minute of incubation, the absorption intensity at 200 nm decreases continuously (Fig. S1a†), reflecting on the concentration of urea in the solution. The lower the concentration in solution, the higher amount of analyte adsorbed into/onto ZIP-8/Ag structure. Thus, when the steady state is reached after 50 min of incubation, the urea concentration in solution is around 31.0 μM, which is 62.0% relative to that of the initial solution. Concerning MB and CR concentration only slightly changed during incubation. MB solution reached the steady state after 30 minutes at the concentration of 48.7 μM, which is 97.4% relative to that of the initial solution. Besides, the steady state of the CR solution was achieved after 20 min of incubation at the concentration of 47.5 μM, which is 95.0% relative to that of the initial solution.

The adsorption capacity of an adsorbate, q_e, which is the amount of the adsorbate adsorbed per unit mass of the adsorbent at the equilibrium state (mg g^{-1}), is usually calculated using the equation:

$$q_e = \frac{(C_i - C_e) \times V}{m} \quad (2)$$

in which C_i and C_e are the initial and equilibrium concentrations of the adsorbate, respectively (mg L^{-1}); V is the solution volume V; and m is the mass of the adsorbent (g).

This equation could be employed to calculate the adsorption capacities of urea, MB and CR into/onto ZIP-8/Ag. C_i is the initial concentration of each analyte, which is 50 μM. The adsorption capacities of urea, MB and CR was estimated to be 22.8 mg g^{-1} ≈ 3.8 × 10^{-4} mol g^{-1}, 8.3 mg g^{-1} ≈ 2.6 × 10^{-5} mol g^{-1} and 34.8 mg g^{-1} ≈ 5 × 10^{-5} mol g^{-1}. Therefore, urea has the largest adsorption capacity, followed by CR and then MB. In another word, on a certain ZIP-8/Ag substrate, the number of urea molecules which can be adsorbed into/onto the substrate is the highest, followed by that of CR and then MB, urea > CR > MB. The difference in adsorption capacity of the three analytes is in correlation with the difference in their SERS enhancement on ZIP-8/Ag. It further confirmed that SERS enhancements achived on ZIP-8/Ag was related to the adsorption of the analytes into/onto the substrate. These differences reminds the distinctions in their properties. To be detailed, every dimension of urea molecule is smaller than the pore size of ZIP-8. It could have allowed it to be adsorbed into the MOF matrix, and locally concentrated within the SERS substrate. In contrast, large molecules with one dimension larger than ZIP-8 pore size could have not been well-adsorbed into the matrix. However, Fig. 5 and the calculated adsorption capacities show that there was still a small amount of MB and CR adsorbed onto the substrate. They could have adsorbed on the surface of the material. It is worth reminding that in solution, CR is negatively charged, thus, it was convenient for it to be adsorbed on the nodes of Zn^{2+} on ZIP-8/Ag. Meanwhile, MB is positively charged, and it could have been adsorbed on citrate-coated AgNPs. Although urea is not charged, it is highly polar. Through ion–dipole forces, urea molecules could have also interacted with Zn^{2+} node to be adsorbed on the surface. However, the adsorption of analyte on the surface of the substrate seemed not to significantly enhance their SERS signal, reflecting in the poor performance to sense MB and CR using ZIP-8/Ag. In addition, to clarify the contribution of surface adsorption of analyte to the SERS enhancement, we destroyed the ZIP-8 frames in ZIP-8/Ag using ultrasonication and employed it as SERS substrate to record SERS spectrum of urea (10^{-3} M) and compare it with SERS spectrum of urea on AgNPs (Fig. 6b). Fig. 6a shows SEM image of ZIP-8 after ultrasonication on the left, displaying that ZIP-8 particles have been broken into fragments. On the right, SEM image of ZIP-8/Ag after ultrasonication exhibit bright particles with the size of 20–30 nm, which could be AgNPs. Furthermore, the image is blurred, which could be due to the presence of organic fragments in the mixture. Eventhough the MOF structure was destroyed, Zn^{2+} still remained in the mixture to interact with urea molecules. However, Fig. 6b shows no significant enhancement in SERS signal of urea on ultrasonication-treated ZIP-8/Ag in comparison to that on AgNPs. Therefore, the impact of analyte adsorption on the surface of urea *via* this interaction was negligible compared to its adsorption into the MOF matrix. Moreover, as the ZIP-8 structure were destroyed, the self assembly of AgNPs could be observed in Fig. 6a (right) with interparticle distance of less than 5 nm, which is similar to our previous reports.[31,41] Therefore, obtained SERS spectra on treated ZIP-8/Ag of all three analytes are similar to those on AgNP. The results of MB (Fig. 6c) and CR (Fig. 6d) reconfirm our hypothesis that by using ZIP-8/Ag, we sacrificed the advantage of AgNP self assembly in the Al substrate. Only if the analyte is small enough to be adsorbed into the MOF matrix to be concentrated, an enhancement in SERS signal can be achieved. This adsorption helps to gather

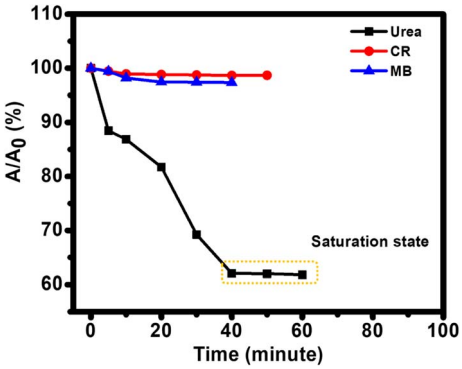

Fig. 5 Changes in relative concentration of urea, MB and CR in the presence of ZIF-8/Ag in solution during incubation time.

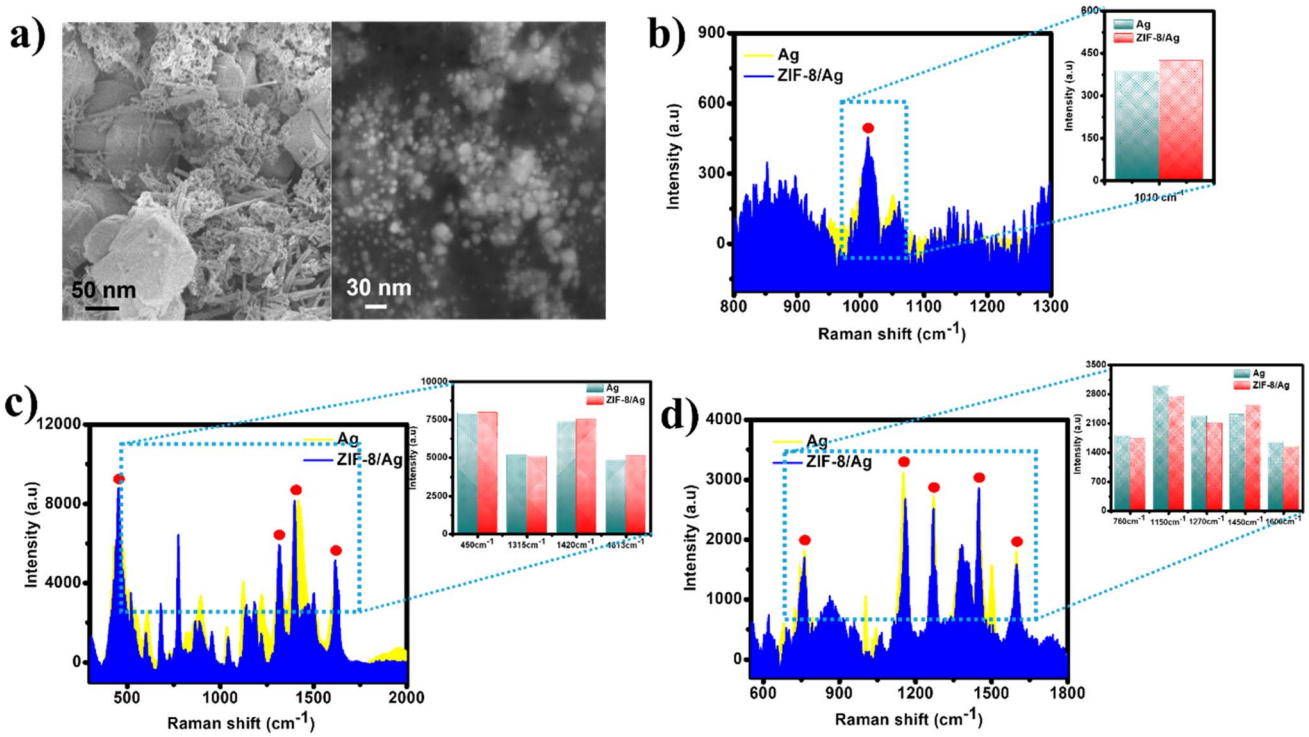

Fig. 6 (a) SEM image of ZIF-8 (left) and ZIF-8/Ag (right) treated with ultrasonication; SERS intensities at characteristic peaks of (b) urea (10^{-3} M), (c), MB (10^{-5} M), and (d) CR (10^{-4} M) on AgNPs and ZIP-8/Ag, in which ZIP-8 frames was destroyed after ultrasonication treatment.

the analyte molecules at a close distance to the AgNPs, which is the centres of SERS effect, allowing the analyte to experience SERS enhancement in both chemical and electromagnetic mechanism. It suggests a size-selection approach, which could be useful to develop applications of ZIP-8/Ag based SERS sensors.

ZIP-8/Ag was then utilized to develop SERS-based sensors for urea detection.

3.3. ZIP-8/Ag-based SERS sensors for urea detection

Fig. 7a demonstrates SERS spectra of urea at eight concentrations (10^{-3} to 10^{-10} M) on ZIP-8/Ag. The presence of the characteristic band of urea at 1010 cm^{-1} could be observed in the SERS spectra with concentrations down to 10^{-9} M. Plot of logarithmic SERS intensity at 1010 cm^{-1} against logarithmic concentration of urea shows a good linear relationship in the region from 10^{-9} M to 10^{-3} M with a linear regression of $R^2 = 0.97$ (Fig. 7b). For each point of the plot, three spectra were collected at three different spots on the SERS substrate. Based on the linear equation shown in Fig. 7b, LOD was calculated to be 1.48×10^{-10} M, which is much more impressive than many reported noble metal-based SERS sensors for urea (Table 1). LOD was calculated as described in ESI.† Besides, the reproducibility of the method was evaluated by measuring SERS signal of urea (10^{-5} M) on 5 ZIP-8/Ag substrates, which were prepared independently using the same protocol, as shown in Fig. 7d. SERS intensities of urea at 1010 cm^{-1} were employed to calculate relative standard deviation (RSD) as shown in ESI.† Thanks to the simplicity of the sample preparation, the reproducibility RSD was estimated to be 13.91%, indicating good reproducibility of the method. In addition, measuring SERS signal of urea on ten different positions on a substrate resulted in similar SERS intensity (Fig. 7c). The uniformity RSD was calculated to be 13.02%.

Table 1 shows that different strategies have been employed to improve the sensing performance of the low Raman cross-section molecule, urea. For example, bimetallic Au@Ag core shelled NPs was prepared to improve the sensitivity, in comparison to the use of pure AuNPs in a study of Hussain *et al.*[42] Besides, AgNPs with sharp tips such as nanodendrite and nanostar were synthesized to create hot spots, amplifying SERS signal of urea.[43,44] In order to forming hot spots, Verma *et al.* decorated AgNPs on fibers of filter paper to enhance SERS signal of urea.[45] Recently, we develop a technique called photo-induced enhanced Raman spectroscopy (PIERS) with the use of Ag-TiO_2, requiring a step of UV pre-irradiation $\lambda = 365$ nm before SERS measurement.[36] The pre-irradiation step causes oxygen vacancies on the surface of TiO_2 semiconductor. Therefore, electrons would jump from the oxygen vacancy states to the conduction band of TiO_2 and then, they are injected to the Fermi level of Ag, leading to the increase in density of density of hot electrons on the surface of AgNPs, allowing more electrons to be transferred to the analyte. Consequently, SERS sensitivity of the sensing system was improved, resulting in an LOD lower than the previously developed ones. In this study, we chose another strategy of enhancing the adsorption level of urea into the substrate using ZIP-8, leading to a huge drop in LOD,

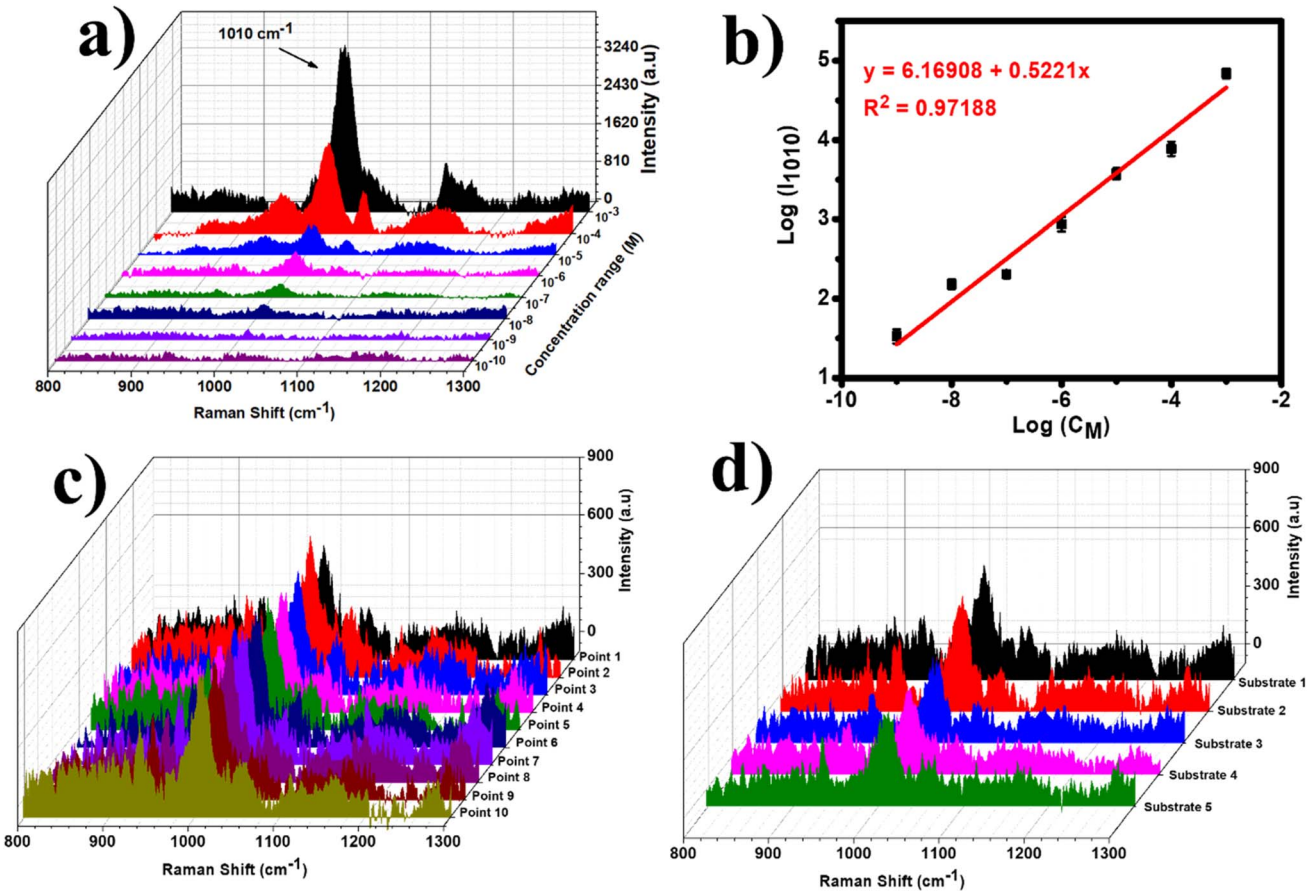

Fig. 7 (a) SERS spectra of urea (10^{-3} M to 10^{-10} M) on ZIF-8/Ag. (b) The plot of the log of SERS intensity at 1010 cm^{-1} against urea concentration. (c) Uniformity and (d) reproducibility of SERS sensors for urea on ZIF-8/Ag substrate.

compared to the others. It emphasizes the importance of adsorption in SERS enhancement.

3.4. Size-selectivity and practicability of ZIP-8/Ag based SERS sensor for urea detection

To confirm the size-selectivity of ZIP-8/Ag based SERS sensors for urea detection, we performed SERS measurements of urea in the presence of CR as an interfering compound. Solutions containing urea and CR were prepared in distilled water with concentrations of 10^{-4} M, 10^{-5} M and 10^{-6} M of each compound. At concentration of 10^{-4} M (Fig. 8a), the presence of urea in the solution is reflected by the appearance of a sharp and intense band at 1010 cm^{-1}. Meanwhile, there is only one characteristic band of CR detected at 1600 cm^{-1}. At concentration of 10^{-5} M (Fig. 8b), with dominant intensity, the band at 1010 cm^{-1} representing the presence of urea can be observed clearly while the band at 1600 cm^{-1} is indistinct with low SERS intensity. Reaching the lowest concentration of 10^{-6} M, there was only urea detected in the solution (Fig. 8c). Therefore, ZIP-8/Ag show size-selectivity while detecting urea in the presence of an interfering compound with one dimension larger than the pore size of the MOF structure.

This size-selectivity is useful for applications of sensors. In this study, we studied the practicability of ZIP-8/Ag based SERS sensor using bottled milk. Milk always contains large molecules such as lipids and proteins leading to high background signal, which could interfere the detection of target analyte. With the

Table 1 Several reported SERS-based urea sensors

Substrate materials	LOD	Linear range	Ref.
Au@AgNP	0.83×10^{-5} M	0.83×10^{-5} to 1.33×10^{-4} M	42
Ag dendrite	3.3×10^{-3} M	3.3×10^{-3} to 1.7×10^{-2} M	43
Au nanostar	3.3×10^{-2} M	3.3×10^{-2} to 3.3×10^{-1} M	44
Ag nanostructures on filter paper	2×10^{-4} M	—	45
Ag-TiO_2 (UV pre-irradiation $\lambda = 365$ nm)	4.6×10^{-6} M	10^{-6} to 10^{-3} M	36
ZIP-8/Ag	1.48×10^{-10} M	10^{-9} to 10^{-3} M	This work

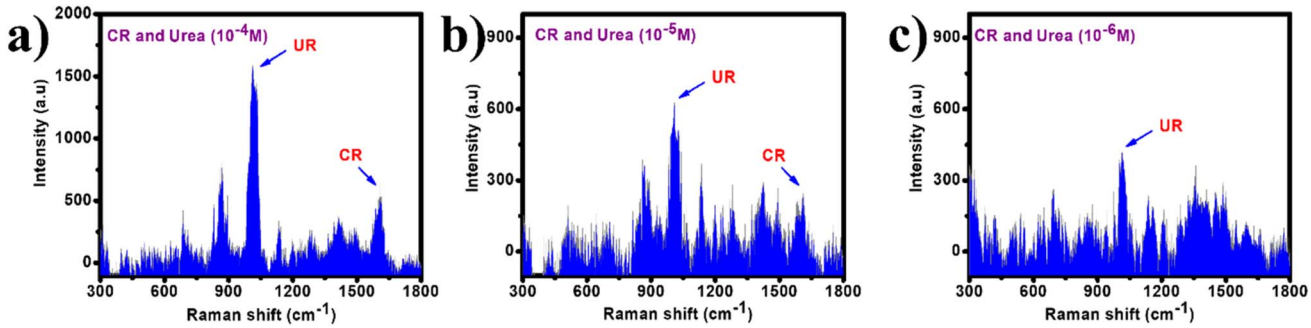

Fig. 8 SERS spectra of solutions containing urea and CR (a) 10^{-4} M, (b) 10^{-5} M, and (c) 10^{-6} M on ZIF-8/Ag.

limited pore size, ZIP-8/Ag could act as a filter, which only allow small molecules to be adsorb inside and experience SERS enhancement. Fig. 9a shows the Raman spectrum of milk (red) and SERS spectrum of milk on ZIP-8/Ag. Raman spectrum exhibits no characteristic band. The SERS spectrum show several peaks, including the intense peak at 250 cm^{-1}, representing the presence of Ag. The other might be related to ZIP-8. However, it is important that there is no intense band around the Raman shift of 1010 cm^{-1}, such as the band at 1003 cm^{-1}, which was assigned to C–H stretching in protein (phenylalanine).[46] Urea was spiked into bottled milk samples to obtain different concentrations (10^{-8} M to 10^{-5} M). SERS measurements of those samples is displayed in Fig. 9b. The characteristic band of urea at 1010 cm^{-1} was detected in every samples down to the concentration of 10^{-8} M. Proteins and other large molecules could have block the pores of MOF and prevent urea to be adsorbed into ZIP-8 as effectively as in standard samples, reducing the accuracy of SERS detecting and sensitivity of the sensors. It results in recovery rates ranging from 88% to 115% (Table S2†). Moreover, the sensor could only detect urea at concentrations down to 10^{-8} M in milk, which is larger than LOD of 1.48 × 10^{-10} M in standard samples. However, the recovery values have been improved compared to our previous study using TiO_2/Ag for urea detection with the recovery rate of 71% to 121%.[36] It could be due to size-selectivity of the sensing system, which reduced interfering noises by preventing adsorption of milk proteins into the SERS substrate. More importantly, ZIP-8/Ag is able to detect the presence of urea in milk at concentrations as low as 10^{-8} M without any pre-treatment on the real samples.

3.5. ZIP-8/Ag as a size-selective SERS substrate for other analytes

To confirm the proposed mechanism of the size-selectivity of the ZIP-8/Ag sensing platform, two other organic compound with different dimensions was selected for SERS measurements. The first one is 4-nitrophenol (4-NP) with the dimensions of 6.6 × 4.3 Å,[47] which are smaller than the pore size of ZIP-8. The second one is chloramphenicol (CAP) with the dimensions of 17.5 × 7.3 × 22.1 Å,[48] among which two dimensions are larger than the MOF pore size. With the dimensions of the two compound, it can be expected that ZIP-8/Ag would improve the

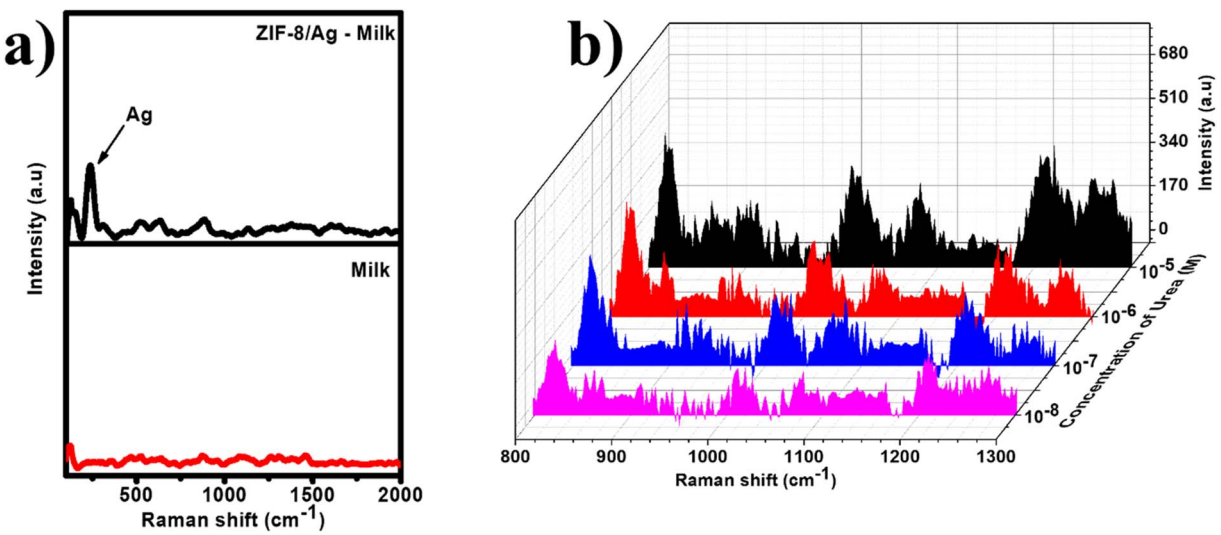

Fig. 9 (a) Raman spectrum of milk (red) and SERS spectrum of milk on ZIF-8/Ag (black); (b) SERS spectra of urea at different concentrations in real samples of milk on ZIF-8/Ag substrates.

SERS performance of sensing 4-NP, compared to the use of pure AgNPs. In contrast, CAP would not be able to be adsorbed into the matrix of ZIP-8/Ag, leading to the lower intensity of SERS signal of CAP on this composite material in comparison to that on AgNPs. Fig. S4† shows SERS spectra of 4-NP at different concentrations (10^{-3} to 10^{-5} M) on ZIP-8/Ag to compare with those on AgNPs. As expected, at every characteristic band, SERS intensity of 4-NP on ZIP-8/Ag is higher that on AgNPs at all concentration. At the lowest concentration of 10^{-5} M, while SERS spectrum of 4-NP on AgNPs does not show any characteristic band, that on ZIP-8/Ag still exhibit sharp and intense peaks, representing the presence of 4-NP. On the other hand, the modification with ZIP-8 does not improve the SERS performance of the SERS substrate for sensing CAP (Fig. S5†). Similar to the results of MB and CR, SERS intensity of CAP on ZIP-8/Ag is lower than that on AgNPs at all characteristic peaks and all concentration. At the lowest concentration of 10^{-5} M, ZIP-8/Ag can not determine the presence of CAP while the other SERS substrate promote the presence of its characteristic peaks. Furthermore, size-selective experiments were also set up using 4-NP and CR (Fig. S6†). Similar to urea, the characteristic peaks of 4-NP can be detected down to concentration of 10^{-6} M. At this concentration, the characteristic peak of CR has disappeared. The additional experiments on other analyte confirm the size-selectivity of ZIP-8/Ag as a SERS based sensing platform. It suggests a step of comparing dimensions of analytes and MOF pore sizes when developing SERS active materials using MOF.

Both urea and 4-NP have dimensions smaller than the pore size of ZIP-8. Therefore, it could be expected that both analytes can be well adsorbed into ZIP-8 structures. Fig. S7† shows SERS spectra of urea and 4-NP in mixed solutions (10^{-4} to 10^{-6} M) on ZIP-8/Ag. The presence of urea can be detected with the band at 1010 cm^{-1}. Meanwhile, the presence of 4-NP is also confirm by characteristic bands. The characteristic bands of 4-NP is listed in Table S3.† SERS intensities of urea at different concentrations in the presence and absence of 4-NP as a interfering molecule are compared in Fig. S8.† The presence of 4-NP has led to a reduction in SERS intensity of urea. However, this reduction is less than 5% at every concentration. Therefore, the presence of small interfering molecule do not lead to significant influence on SERS performance of ZIP-8/Ag-based sensor for urea.

4. Conclusions

In this study, we fabricated ZIP-8/Ag nanocomposite using simple physical mixing method. The nanocomposite was employed as SERS substrates for detection of different analytes with distinct dimensions, including urea, MB and CR, among which urea has every dimensions smaller than the pore size of ZIP-8 while the others has one dimension larger than that. The dimensions of analyte exhibit obvious effect on their ability to be adsorbed into/onto the SERS substrate as well as the SERS performance. With appropriate dimensions, urea was the only analyte adsorbed effectively into ZIP-8/Ag, leading to significant improvements in SERS performance of the sensing systems. ZIP-8/Ag, therefore, worked as a filter in a size-selective SERS sensing platform. ZIP-8/Ag based SERS sensor could detect urea at concentrations down to 1.48×10^{-10} M in standard solutions and 10^{-8} M in milk samples. The size-selectivity was re-confirmed with two other analytes: a small one, 4-NP, and a large one, CAP. The results were in good agreement with the expectation that only 4-NP achieved large SERS enhancements on ZIP-8/Ag. It suggests a simple step of comparing dimensions of target molecules and MOF pore sizes before developing SERS active materials using MOF nanostructures to optimize their SERS performance.

Data availability

The data supporting this article have been included as part of the ESI.†

Author contributions

D. T. N. Nga: conceptualization, validation, investigation, writing-original draft; Q. D. Mai: conceptualization, validation, investigation; N. H. T. Linh: validation, investigation; D. L. H. Tan: validation, investigation, methodology; V. T. K. Oanh: validation, investigation; T. N. Bach: validation, investigation; V. D. Lam: methodology, validation, formal analysis; H. A. Nguyen: conceptualization, methodology, formal analysis, writing-review & editing; A. T. Le: conceptualization, methodology, supervision, project administration, writing-review & editing.

Conflicts of interest

The authors declare that they have no known competing financial interests or personal relationships that could have appeared to influence the work reported in this paper.

Acknowledgements

This research is funded by Phenikaa University under grant number PU2024-1-A-03 and also partially supported by the Vietnam National University, Ho Chi Minh City under grant number TX2024-50-01 for the ZIP-8 synthesis and characterization. The authors would like to acknowledge the support for Raman & UV-vis measurements from NEB Lab in the Phenikaa University, and SEM analysis from IOP-VAST, Vietnam.

References

1 H. M. Lee, S. M. Jin, H. M. Kim and Y. D. Suh, *Phys. Chem. Chem. Phys.*, 2013, **15**, 5276–5287.
2 A. I. Pérez-Jiménez, D. Lyu, Z. Lu, G. Liu and B. Ren, *Chem. Sci.*, 2020, **11**, 4563–4577.
3 Y. Chen, Y. Tang, P. Li, Y. Wang, Y. Zhuang, S. Sun, D. Wang and W. Wei, *Anal. Chim. Acta*, 2023, **1278**, 341739.
4 W. Na, C. Ou, Y. Ming, Y. Gao and L. Tian, *Sens. Actuators, B*, 2023, **385**, 133725.
5 R. Pilot, R. Signorini, C. Durante, L. Orian, M. Bhamidipati and L. Fabris, *Biosensors*, 2019, **9**, 57.

6 L. Jensen, C. M. Aikens and G. C. Schatz, *Chem. Soc. Rev.*, 2008, **37**, 1061–1073.
7 G. C. Olar, L. C. Cotet, L. Baia, A. Mihis and M. Baia, *Mater. Today: Proc.*, 2021, **45**, 4096–4099.
8 Y. Han, X. Fang, Z. Sun, C. Kang, L. Zha and X. Zhang, *ACS Appl. Nano Mater.*, 2022, **5**, 2445–2450.
9 Y. Zhang, R. J. Liu, X. Ma, X. Y. Liu, Y. X. Zhang and J. Zhang, *RSC Adv.*, 2018, **8**, 37750–37756.
10 Q. Wang, R. Hu, M. Chen, J. Zhang, L. Chen, Z. Lin, Y. Dong and F. Fu, *Anal. Chem.*, 2021, **93**, 9744–9751.
11 A. K. Pal, S. Pagal, K. Prashanth, G. K. Chandra, S. Umapathy and D. B. Mohan, *Sens. Actuators, B*, 2019, **279**, 157–169.
12 M. Kadir, R. Nemkayeva, G. Baigarinova, B. Alpysbayeva, A. Assembayeva and V. Smirnov, *Phys. E*, 2023, **145**, 115499.
13 O. M. Yaghi, M. O'Keeffe, N. W. Ockwig, H. K. Chae, M. Eddaoudi and J. Kim, *Nature*, 2003, **423**, 705–714.
14 H. Furukawa, K. E. Cordova, M. O'Keeffe and O. M. Yaghi, *Science*, 2013, **341**, 1230444.
15 I. Ihsanullah, *Curr. Opin. Environ. Sci. Health*, 2022, **26**, 100335.
16 M. Wen, G. Li, H. Liu, J. Chen, T. An and H. Yamashita, *Environ. Sci.:Nano*, 2019, **6**, 1006–1025.
17 B. Li, H.-M. Wen, W. Zhou and B. Chen, *J. Phys. Chem. Lett.*, 2014, **5**, 3468–3479.
18 X. Zhang, P. Liu and Y. Zhang, *Inorg. Chim. Acta*, 2023, **557**, 121683.
19 Y. Cai, Y. Wu, T. Xuan, X. Guo, Y. Wen and H. Yang, *ACS Appl. Mater. Interfaces*, 2018, **10**, 15412–15417.
20 Q.-Q. Chen, R.-N. Hou, Y.-Z. Zhu, X.-T. Wang, H. Zhang, Y.-J. Zhang, L. Zhang, Z.-Q. Tian and J.-F. Li, *Anal. Chem.*, 2021, **93**, 7188–7195.
21 J. Yang, M. Pan, X. Yang, K. Liu, Y. Song and S. Wang, *Food Chem.*, 2022, **395**, 133623.
22 K. Huang, S. Gong, L. Zhang, H. Zhang, S. Li, G. Ye and F. Huang, *Chem. Commun.*, 2021, **57**, 2144–2147.
23 Q. Li, S. Gong, H. Zhang, F. Huang, L. Zhang and S. Li, *Chem. Eng. J.*, 2019, **371**, 26–33.
24 Y. Zhang, C. Xue, P. Li, S. Cui, D. Cui and H. Jin, *J. Hazard. Mater.*, 2022, **424**, 127686.
25 C. Tanford, *Science*, 1986, **233**, 898.
26 M. Arias, E. López, A. Nuñez, D. Rubinos, B. Soto, M. T. Barral and F. Díaz-Fierros, in *Effect of Mineral-Organic-Microorganism Interactions on Soil and Freshwater Environments*, ed. J. Berthelin, P. M. Huang, J. M. Bollag and F. Andreux, Springer US, Boston, MA, 1999, pp. 361–365, DOI: 10.1007/978-1-4615-4683-2_39.
27 R. W. Dapson, *Biotech. Histochem.*, 2018, **93**, 543–556.
28 D. T. Nguyen, L. D. T. Nguyen, Q. T. Pham, T. M. Le, B. Q. G. Le, N. X. D. Mai, T. L. H. Doan and L. H. T. Nguyen, *Microporous Mesoporous Mater.*, 2021, **327**, 111445.
29 P. Utpalla, S. K. Sharma, J. Mor, J. Prakash, J. Bahadur and P. K. Pujari, *Microporous Mesoporous Mater.*, 2021, **327**, 111409.
30 T. A. Makhetha, S. C. Ray and R. M. Moutloali, *ACS Omega*, 2020, **5**, 9626–9640.
31 M. Q. Doan, N. H. Anh, N. X. Quang, N. X. Dinh, D. Q. Tri, T. Q. Huy and A.-T. Le, *J. Electron. Mater.*, 2022, **51**, 150–162.
32 V. Q. Khue, T. Q. Huy, V. N. Phan, A. Tuan-Le, D. T. Thanh Le, M. Tonezzer and N. T. Hong Hanh, *Mater. Chem. Phys.*, 2020, **255**, 123562.
33 D. T. Thuc, T. Q. Huy, L. H. Hoang, B. C. Tien, P. Van Chung, N. T. Thuy and A.-T. Le, *Mater. Lett.*, 2016, **181**, 173–177.
34 S. Tanaka, K. Fujita, Y. Miyake, M. Miyamoto, Y. Hasegawa, T. Makino, S. Van der Perre, J. Cousin Saint Remi, T. Van Assche, G. V. Baron and J. F. M. Denayer, *J. Phys. Chem. C*, 2015, **119**, 28430–28439.
35 S. Ben-Jaber, W. J. Peveler, R. Quesada-Cabrera, E. Cortés, C. Sotelo-Vazquez, N. Abdul-Karim, S. A. Maier and I. P. Parkin, *Nat. Commun.*, 2016, **7**, 12189.
36 Q. D. Mai, H. A. Nguyen, T. L. H. Phung, N. Xuan Dinh, Q. H. Tran, T. Q. Doan, A. T. Pham and A.-T. Le, *ACS Appl. Nano Mater.*, 2022, **5**, 15518–15530.
37 C. Ruan, G. Eres, W. Wang, Z. Zhang and B. Gu, *Langmuir*, 2007, **23**, 5757–5760.
38 G.-N. Xiao and S.-Q. Man, *Chem. Phys. Lett.*, 2007, **447**, 305–309.
39 L. Zhong, Y. Hu and D. Xing, Adsorption orientation of methylene blue (MB+) on the silver colloid: SERS and DFT studies, *2009 Conference on Lasers & Electro Optics & the Pacific Rim Conference on Lasers and Electro-Optics*, 2009, pp. 1–2.
40 M. L. de Souza, D. C. Tristão and P. Corio, *RSC Adv.*, 2014, **4**, 23351–23358.
41 D. T. Linh, Q.-D. Mai, D. T. Nguyet Nga, N. T. Anh, H. Van Tuan, H. A. Nguyen, X. H. Vu and A.-T. Le, *RSC Adv.*, 2024, **14**, 9975–9984.
42 A. Hussain, D.-W. Sun and H. Pu, *Food Addit. Contam.,:Part A*, 2019, **36**, 851–862.
43 J. Wen, F. Song, Y. Du, W. Yu and R. Qiang, *IOP Conf. Ser.:Mater. Sci. Eng.*, 2019, **688**, 033040.
44 P. S. Menon, F. A. Said, G. S. Mei, D. D. Berhanuddin, A. A. Umar, S. Shaari and B. Y. Majlis, *PLoS One*, 2018, **13**, e0201228.
45 M. Verma, T. K. Naqvi, S. K. Tripathi, M. M. Kulkarni and P. K. Dwivedi, *Environ. Technol. Innovation*, 2021, **24**, 102033.
46 I. W. Schie and T. Huser, *Appl. Spectrosc.*, 2013, **67**, 813–828.
47 M. A. Adebayo and F. I. Areo, *Resour. Environ. Sustain.*, 2021, **3**, 100020.
48 C. Chatterjee, J. K. Dattagupta, N. N. Saha, W. Saenger and K. Müller, *J. Cryst. Mol. Struct.*, 1979, **9**, 295–304.